arXiv:1611.03077v1 [nucl-th] 9 Nov 2016

The comparative effect of an addition of a surface term to the Woods-Saxon potential on the thermodynamics of a nucleon

B.C. Lütfüoğlu

*Department of Physics, Akdeniz University, 07058 Antalya, Turkey**

M. Erdogan

Department of Physics, Namik Kemal University, 59030 Tekirdag, Turkey

(Dated: November 10, 2016)

Abstract

Our main motivation in this work is to compare physical consequences of the two potentials in context of quantum mechanics and statistical thermodynamics.

In this study, we reveal the difference between Woods-Saxon (WS) and Generalized Symmetric Woods-Saxon (GSWS) potentials in order to describe the physical properties of a nucleon, by means of solving Schrödinger equation for the two potentials. The additional term squeezes the WS potential well, which leads an upward shift in the spectrum, resulting in a more realistic picture. The resulting GSWS potential does not merely accommodate extra quasi bound states, but also has modified bound state spectrum. As an application, we apply the formalism to a real problem, an α particle confined in Bohrium-270 nucleus. The thermodynamic functions Helmholtz energy, entropy, internal energy, specific heat of the system are calculated and compared in both wells. The internal energy and the specific heat capacity increase, as a result of upward shift in the spectrum. The shift of the Helmholtz free energy is a direct consequence of the shift of the spectrum. The entropy decreases because of a decrement in the number of available states.

PACS numbers: 03.65.-w, 03.65.Ge, 05.30.-d

Keywords: Woods-Saxon potential, generalized symmetric Woods-Saxon potential, bound states, analytical solutions, partition function, thermodynamic functions

* bclutfuoglu@akdeniz.edu.tr

I. INTRODUCTION

In recent years, the thermodynamic functions gained popularity, in order to understand the physical properties of numerous potentials in relativistic or non-relativistic regimes. Hassanabadi *et al.* studied thermodynamic properties of the 3D Dirac Oscillator with Aharonov-Bohm field and magnetostatic monopole potential [1]. Pacheco *et al.* analyzed one-dimensional Dirac oscillator in a thermal bath and they showed that its heat capacity is two times greater than that of the one-dimensional harmonic oscillator for high temperatures [2]. Franco-Villafañe *et al.* is performed the first experimental study on one-dimensional Dirac oscillator [3]. Later, Pacheco *et al.* also studied three dimensional Dirac oscillator in a thermal bath [4]. They reported that the degeneracy of energy levels and their physical implications implied that, at high temperatures, the limiting value of the specific heat is three times bigger than that of the one dimensional case. Boumali studied the properties of the thermodynamic quantities of the relativistic harmonic oscillator using the Hurwitz zeta function. He compared his results with those obtained by a method based on the Euler-MacLaurin approach [5]. Boumali also showed that, with the concept of effective mass, the model of a two dimensional Dirac oscillator can be used to describe the thermal properties of graphene under a uniform magnetic field, where all thermodynamic properties of graphene were calculated using the zeta function [6]. He also studied the thermodynamics of the one-dimensional Duffin-Kemmer-Petiau oscillator via the Hurwitz zeta function method [7] in which study, he calculated the free energy, the total energy, the entropy, and the specific heat. Larkin *et al.* have studied thermodynamics of relativistic Newton-Wigner particle in external potential field [8]. Vincze *et al.* investigated Nonequilibrium Thermodynamic and Quantum Model of a Damped Oscillator [9]. Arda *et al.* studied thermodynamic quantities such as the mean energy, Helmholtz free energy, and the specific heat with the Klein-Gordon, and Dirac equations [10]. Dong *et al.* studied hidden symmetries and thermodynamic properties for a harmonic oscillator plus an inverse square potential [11].

The WS potential well [12] is widely employed to model the physical systems in nuclear [12–21], atom-molecule [21, 22], relativistic [23–31] and non-relativistic [32–37] physics problems.

The energy barrier at the surface of atomic nucleus that nucleons are exposed, various type of additional terms to WS potential are proposed to produce GSWS potentials. Such

potential wells can be used to model any system, in which a particle is trapped in a finite space, as well as the effects, such as non-zero l, spin-orbit coupling [38–55].

Our main motivation in this work is to compare physical consequences of the two potentials in context of quantum mechanics and statistical thermodynamics. We consider the physical properties of α particle as an application, to reinforce the formal treatment of the two potentials for Bh-270 nucleus.

In section II, we interpret the forms of the WS and GSWS potentials, and corresponding energy eigenvalues, for a massive non-relativistic confined particle, using the formalism proposed by [41]. In section III, we give a brief summary on the thermodynamic functions, that are calculated in the following section for the two potentials. In section IV, the energy spectra of α particle in Bh-270 nucleus for the two potentials are presented as an application of the formalism presented, upon which, the thermodynamic functions of the system are plotted and discussed in terms of the parameters of the problem. In section V, the conclusion is given.

II. THE MODEL

The WS potential well in one dimension is described by

$$V(x) = -\theta(-x)\frac{V_0}{1+e^{-a(x+L)}} - \theta(x)\frac{V_0}{1+e^{a(x-L)}}, \tag{1}$$

where $\theta(\pm x)$ are the Heaviside step functions, a is the reciprocal of the diffusion coefficient, L measures the size of the nucleus, V_0 is the depth of the potential, given by [14]

$$V_0 = 40.5 + 0.13A, \tag{2}$$

where A is the atomic number of the nucleus.

According to the assumption that a nucleon suffers a potential barrier when near the surface of its nucleus or being emitted to outside, the WS potential is considered inadequate to explain the dynamics of this type of problems. In order to take the surface effect into account, an additional term to the WS potential is widely used [39–41]. The WS potential

combined with the additional terms are called GSWS potential.

$$V(x) = \theta(-x)\left[-\frac{V_0}{1+e^{-a(x+L)}} + \frac{W_0 e^{-a(x+L)}}{\left(1+e^{-a(x+L)}\right)^2} \right] + \theta(x)\left[-\frac{V_0}{1+e^{a(x-L)}} + \frac{W_0 e^{a(x-L)}}{\left(1+e^{a(x-L)}\right)^2} \right], \tag{3}$$

here the second terms in the brackets correspond to the energy barrier that nucleon faces at the surface, which is taken as linearly proportional to the spatial derivative of the first term multiplied by the nuclear size. The unitless proportionality multiplier, hereby ρ, which is implicitly included in W_0, can be calculated via conservation laws.

Because of the symmetry of the potential, even E_n^e and odd E_n^o energy eigenvalues arise, which are studied extensively in the reference [41] and evaluated to be

$$E_n^e = -V_0 + \frac{\hbar^2}{2mL^2}\left| \arctan\frac{(N_1-N_2)}{i(N_1+N_2)} \pm n'\pi \right|^2, \tag{4}$$

$$E_n^o = -V_0 + \frac{\hbar^2}{2mL^2}\left| \arctan\frac{(N_1+N_2)}{i(N_1-N_2)} \pm n'\pi \right|^2, \tag{5}$$

here n' are integers, whereas n stands for the number of nodes, the roots of the wave functions. N_1 and N_2 are complex numbers

$$N_1 = \frac{\Gamma(c_1)\Gamma(c_1-a_1-b_1)}{\Gamma(c_1-a_1)\Gamma(c_1-b_1)}, \tag{6}$$

$$N_2 = \frac{\Gamma(c_1)\Gamma(a_1+b_1-c_1)}{\Gamma(a_1)\Gamma(b_1)}, \tag{7}$$

and implicitly dependent on energy eigenvalues via the coefficients a_1, b_1 and c_1

$$a_1 = \mu + \theta + \nu, \tag{8}$$

$$b_1 = 1 + \mu - \theta + \nu, \tag{9}$$

$$c_1 = 1 + 2\mu, \tag{10}$$

here

$$\mu = \sqrt{-\frac{2mE_n}{a^2\hbar^2}}, \tag{11}$$

$$\nu = \sqrt{-\frac{2m(E_n+V_0)}{a^2\hbar^2}}, \tag{12}$$

$$\theta = \frac{1}{2} \mp \sqrt{\frac{1}{4} - \frac{2mW_0}{a^2\hbar^2}}. \tag{13}$$

When $W_0 = 0$, N_1 and N_2 remain unchanged because of the symmetry in the multiplication of the Gamma functions under the possible values of θ, which are either 0 or 1. Moreover, since the whole energy spectrum is negative, μ is real, the ordinary solutions for the WS potential are obtained. When W_0 is between 0 and V_0, the WS potential well is slightly modified, because of being narrower, but not yet giving rise to positive energy eigenvalues. When W_0 exceeds V_0, the barrier starts to grow and the well keeps narrowing, this alters the energy spectrum, including an extension to positive values. The positive energies are the reason for complex values of μ, which are responsible for tunnelling occurring in some nuclei. These states are called quasi-bound states.

The energy spectrum of a nucleon under GSWS potential is composed of energy eigenvalues, satisfying

$$-V_0 < E_n < V_0 \frac{(1-\rho aL)^2}{4\rho aL} \tag{14}$$

then, ν can take only imaginary values for the entire scope of the spectrum.

III. THERMODYNAMICS OF A SYSTEM

Exploiding the energy spectrum, the partition function of the system is given by

$$Z(\beta) = \sum_n e^{-\beta E_n}, \tag{15}$$

where β is defined by

$$\beta = \frac{1}{k_B T}. \tag{16}$$

and k_B stands for the Boltzman constant, T is the temperature in the unit of Kelvin. The Helmholtz free energy of the system can be calculated using the equation

$$F(T) \equiv -k_B T \ln Z(\beta). \tag{17}$$

The entropy of the system is given by,

$$S(T) = -\frac{\partial}{\partial T} F(T). \tag{18}$$

The internal energy $U(T)$ is the expectation value of the energy of the system

$$U(T) = -\frac{\partial}{\partial \beta} \ln Z(\beta). \tag{19}$$

Then, the isochoric specific heat capacity $C_v(T)$ is defined by

$$C_v(T) \equiv \frac{\partial}{\partial T} U(T). \tag{20}$$

IV. AN APPLICATION OF THE FORMALISM FOR BH-270 NUCLEUS

In this section we present the thermodynamic treatment of an α particle within Bh-270 nucleus as an application of the formalism described in previous sections, in order to investigate the effects of the surface term addition to the WS potential. For this nucleus, in ref [14] the inverse diffusion parameter is given as $a = 1.538 fm^{-1}$, while the radius is evaluated to be $L = 8.068 fm$. Substituting the atomic number $A = 270$ into Equation 2, we have $V_0 = 75.617 MeV$ and then $W_0 = 215.523 MeV$.

The corresponding WS and GSWS potentials are shown in Figure 1. The calculated energy spectra of an α particle with mass $m = 3727.379 MeV/c^2$ in the nucleus are tabulated in Table I and Table II for WS and GSWS, respectively. Purely real bound state energy eigenvalues in both spectra imply infinite time constants, which mean zero decay probability for the nucleon from the nucleus. Whereas, the quasi-bound states in the GSWS spectrum have a complex form with finite time constants, which are responsible for the decay probability [56, 57].

Using the partition function given in Equation 15, the Helmholtz and the entropy functions versus reduced temperature curves of the system, corresponding to the cases of GS and GSWS potentials are presented in Figure 2 (a) and (b), respectively. The entropy in both cases start from zero, being in agreement with the third law of thermodynamics. The saturation values of the entropy are $2.66 \times 10^{-10} MeV/K$ and $2.62 \times 10^{-10} MeV/K$ for WS and GSWS potentials, respectively. Surprisingly the addition of the the surface term does not lead to an increase in the number of available states, contrarily, it results in a decrease in the number of available states from 22 to 21. This is a consequence of the upper shift of the energy spectrum by *squeezing* the well with the addition. The increase of the Helmholtz free energy is due to the upward shift in the energy spectrum.

In Figure 3, the internal energy $U(T)$ functions are shown as functions of reduced temperature for the WS and GSWS potential wells. When the surface terms are introduced, positive energy eigenvalues appear, while the number of negative energy eigenvalues decrease, accompanied by an upward shift in the energy spectrum. All these modifications in

the spectrum give rise to an increase in the internal energy, as indicated in the Figure 3. The internal energies initiate at the values $-75.283MeV$ and $-75.166MeV$ at $0K$ for the WS and GSWS potentials, which are the lowest energy eigenvalues in the spectra, respectively. These internal energies are not distinguishable to the naked eye until the reduced temperature of about 0.007, at which the difference broadens, as observed in Figure 3 (b). The limiting values of the internal energies of the two cases goes to the mean values of the $-42.586MeV$ and $-35.535MeV$ for the spectra of WS and GSWS, respectively, as the reduced temperature goes to infinity.

In Figure 4, the specific heat $C_v(T)$ versus reduced temperature curves are demonstrated. The steep linear initial increase is a consequence of the initial convex behavior of the internal energies, which is a common characteristics of the two cases. After that, $C_v(T)$ remains constant, followed by a decay to zero, in the whole scale of the reduced temperature. The specific heat function for GSWS potential has higher values during this decay, which verifies that the internal energy saturates to a higher value at higher reduced temperature.

V. CONCLUSION

In this study, we analyze the effect of the additional term, representing the surface effect of a nucleus, to WS potential well. We formally discuss how the additional term modifies the whole non-relativistic energy spectrum by squeezing the well, resulting in an upward shift of the spectrum. GSWS potential does not merely accommodate extra quasi bound states, but also has modified bound state spectrum. As an application of the formal treatment, we consider α particle inside Bh-270 nucleus, modeled with both WS and GSWS potential wells. The thermodynamic functions Helmholtz free energy, entropy, internal energy, specific heat are calculated in both approaches and compared. The internal energy and the specific heat capacity increase, as a result of upward shift in the spectrum. The shift of the Helmholtz free energy is a direct consequence of the shift of the spectrum. The entropy decreases due to the decrement in the number of available states, which arises as a result of narrowing the well with the additional term. It is concluded that GSWS potential is more realistic to describe the physical properties of α particle within Bh-270 nucleus.

ACKNOWLEDGMENTS

This work was partially supported by the Turkish Science and Research Council (TÜBİTAK) and Akdeniz University. The authors would like to thank to Dr. E. Pehlivan for his valuable assistance.

VI. REFERENCES

[1] Hassanabadi H, Sargolzaeipor S., Yazarloo B.H. 2015 Thermodynamic Properties of the Three-Dimensional Dirac Oscillator with Aharonov-Bohm Field and Magnetic Monopole Potential. *Few-Body Syst.* **56**, 115-124.

[2] Pacheco M H, Landim R R, Almeida C A S. 2003 One-dimensional Dirac oscillator in a thermal bath. *Phys. Lett. A* **311**, 93-96.

[3] Franco-Villafañe J A, Sadurní E, Barkhofen S, Kuhl U, Mortessagne F, Seligman T H 2013 First Experimental Realization of the Dirac Oscillator. *Phys. Rev. Lett.* **111**, 170405.

[4] Pacheco M H, Maluf R V, Almeida C A S 2014 Three-dimensional Dirac oscillator in a thermal bath. *EPL* **108**, 10005.

[5] Boumali A 2015 The One-dimensional Thermal Properties for the Relativistic Harmonic Oscillators. *EJTP* **12**, 121-130.

[6] Boumali A 2015 Thermodynamic properties of the graphene in a magnetic field via the two dimensional Dirac oscillator. *Phys. Scr.* **90**, 045702, (109501 Corrigendum).

[7] Boumali A 2015 Thermal Properties of the One-Dimensional Duffin-Kemmer-Petiau Oscillator Using Hurwitz Zeta Function., *Z. Naturforsch A.* **70**, 867-874.

[8] Larkin A. S., Filinov V S 2015 Thermodynamics of relativistic Newton-Wigner particle in external potential field., *Journal of Physics: Conference Series* **653**, 012114.

[9] Vincze G., Szasz A., 2015 *Recent Advances in Thermo and Fluid Dynamics: Chapter 3* (In-Tech, 2015) p. 39-80.

[10] Arda A, Tezcan C, Sever R 2016 Klein-Gordon and Dirac Equations with Thermodynamic Quantities. *Few-Body Syst.* **57**, 93-101.

[11] Dong S H, Lozada-Cassou M, Yu J, Jimenez-Angeles F, Rivera A L 2007 Hidden Symmetries and Thermodynamic Properties for a Harmonic Oscillator Plus an Inverse Square Potential. *Int. J. Quantum Chem.* **107**, 366-371.

[12] Woods R D, Saxon D S 1954 Diffuse Surface Optical Model for Nucleon-Nuclei Scattering. *Phys. Rev.* **95**, 577-578.

[13] Zaichenko A K, Ol'khovskii V S 1976 Analytic solutions of the problem of scattering by potentials of the Eckart class. *Theor. Math. Phys.* **27**, 475-477.

[14] Perey C M, Perey F G, Dickens J K, Silva R J 1968 $11-MeV$ Proton Optical-Model Analysis. *Phys. Rev.* **175**, 1460-1475.

[15] Schwierz N, Wiedenhöver I, Volya A 2007 Parameterization of the Woods-Saxon Potential for Shell-Model Calculations *arXiv:0709.3525*

[16] Michel N, Nazarewicz W, Ploszajczak M, Bennaceur K 2002 Gamow Shell Model Description of Neutron-Rich Nuclei. *Phys. Rev. Lett.* **89**, 042502.

[17] Michel N, Nazarewicz W, Ploszajczak 2004 Proton-neutron coupiling in the Gamow shell model: The lithium chain. *Phys. Rev. C* **70**, 064313.

[18] Esbensen H, Davids C N 2000 Couples-channels treatment of deformed proton emitters. *Phys. Rev. C* **63**, 014315.

[19] Ikhdair S. M., Falaye B. J., Hamzavi M. 2013 Approximate Eigensolutions of the Deformed Woods-Saxon Potential via AIM *Chin.Phys. Lett.* **30**, 020305.

[20] Gautam M. S., Sharma M. K., 2014 Sub barrier fusion of 1632S + 4094Zr system and energy dependent Woods-Saxon potential. 2014 *Proceedings of the DAE Symp. on Nucl. Phys.* **59**, 452-453.

[21] Brandan M E, Satchler G R 1997 The interaction between light heavy-ions and what it tells us. *Phys. Reports* **285**, 143-243.

[22] Satchler G R 1991 Heavy-ion scattering and reactions near the Coulomb barrier and "threshold anomalies". *Phys. Reports* **199**, 147-190.

[23] Kennedy P 2002 The Woods-Saxon potential in the Dirac equation. *J. Phys. A: Math. Gen.* **35**, 689-698.

[24] Panella O, Biondini S, Arda A 2010 New exact solution of the one-dimensional Dirac equation for the Woods-Saxon potential within the effective mass case. *J. Phys. A:Math. Theor.* **43**, 325302.

[25] Aydoğdu O, Arda A, Sever R 2012 Effective-mass Dirac equation for Woods-Saxon potential: Scattering, bound states, and resonances. *J. Math. Phys.* **53**, 042106.

[26] Guo J Y, Sheng Z Q 2005 Solution of the Dirac equation for the Woods-Saxon potential with spin and pseudospin symmetry. *Phys. Lett.* **A338**, 90-96.

[27] Guo J Y, Zheng F X, Fu-Xin X 2002 Solution of the relativistic Dirac-Woods-Saxon problem. *Phys. Rev.* **A66**, 062105.

[28] Rojas C, Villalba V M 2005 Scattering of a Klein-Gordon particle by a Woods-Saxon potential. *Phys. Rev.* **A71**, 052101.

[29] Hassanabadi H, Maghsoodi E, Zarrinkamar S, Salehi N 2013 Scattering of Relativistic Spinless Particles by the Woods-Saxon Potential *Few-Body Syst.* **54**, 2009-2016.

[30] Yazarloo B H, Mehraban H 2016 The Relativistic Transmission and Reflection Coefficients for Woods-Saxon potential. *Acta Phys. Pol. A* **129**, 1089.

[31] Chargui Y 2016 Effective Mass and Pseudoscalar Interaction in the Dirac Equation with Woods-Saxon Potential. *Few-Body Syst.* **57**, 289-306.

[32] Pahlavani M R, Alavi S A 2012 Solutions of Woods-Saxon Potential with Spin-Orbit and Centrifugal Terms through Nikiforov-Uvarov Method. *Commun. Theor. Phys.* **58**, 739-743.

[33] Costa L S, Prudente F V, Acioli P H, Soares Neto J J, Vianna J D M 1999 A study of confined quantum systems using the Woods-Saxon potential. *J. Phys. B: At. Mol. Opt. Phys.* **32**, 2461-2470.

[34] Flügge S 1994 *Practical Quantum Mechanics Vol. I* (Berlin: Springer).

[35] Saha A, Das U, Talukdar 2011 On eigenvalue problems in quantum mechanics. *Phys. Scr.* **83**, 065003(6pp).

[36] Feizi H, Rajabi A A, Shojaei M R 2011 Supersymmetric solution of the Schrödinger equation for Woods-Saxon equation by using the Pekeris Approximation. *Acta Phys. Polon. B* **42**, 2143-2152.

[37] Niknam A, Rajabi A A, Solaimani M 2016 Solutions of D-dimensional Schrodinger equation for Woods-Saxon potential with spin-orbit, coulomb and centrifugal terms through a new hybrid numerical fitting Nikiforov-Uvarov method. *J. Theor. Appl. Phys.* **10**, 53-59.

[38] Candemir N, Bayrak O 2014 Bound states of the Dirac equation for the generalized Woods-Saxon potential in pseudospin and spin symmetry limits. *Mod. Phys. Lett.* **A29**, 1450180.

[39] Bayrak O, Aciksoz E 2015 Corrected analytical solution of the generalized Woods-Saxon potential for arbitrary ℓ states. *Phys. Scr.* **90**, 015302.

[40] Bayrak O, Sahin D 2015 Exact Analytical Solution of the Klein-Gordon Equation in the Generalized Woods-Saxon potential *Commun. Theor. Phys.* **64** 259-262.

[41] Lütfüoğlu B C, Akdeniz F, Bayrak O 2016 Scattering, bound, and quasi-bound states of the generalized symmetric Woods-Saxon potential *J. Math. Phys.* **57**, 032103.

[42] Liendo J A, Castro E, Gomez R and Caussyn D D 2016 A study of Shell Model Neutron States in $^{207,209}Pb$ Using the Generalized Woods-Saxon plus Spin-Orbit Potential *Int. J. Mod. Phys. E* **225**, 1650055

[43] Berkdemir C, Berkdemir A, Sever R 2005 Polynomial solutions of the Schrödinger equation for the generalized Woods-Saxon potential. *Phys. Rev. C* **72**, 027001, errata **74**, 027001 (2005).

[44] Badalov V H, Ahmadov H I, Ahmadov A I 2009 Analytical solutions of the Schrodinger equation with the Woods-Saxon potential for arbitrary l state. *Int. J. Mod. Phys. E* **18**, 631.

[45] Gönül B, Köksal K 2007 A note on the Woods-Saxon potential. *Phys. Scripta* **76**, 565.

[46] Koura H, Yamada M 2000 Single-particle potentials for spherical nuclei. *Nucl. Phys. A* **671**, 96-118.

[47] Çapak M, Petrellis D, Gönül B, Bonatsos D 2015 Analytical solutirons for the Bohr Hamiltonian with the Woods-Saxon potential. *J. Phys. G* **42**, 95102.

[48] Çapak M, Gönül B 2016 Remarks on the Woods-Saxon potential. *Mod. Phys. Lett. A* **31**, 1650134.

[49] Ikot A N, Akpan I O 2012 Bound State Solutions of the Schrödinger Equation for a More General Woods-Saxon Potential with Arbitrary $l-$state. *Chin. Phys. Lett.* **29**, 090302.

[50] Ikhdair S M, Falaye B J, Hamzavi M 2013 Approximate Eigensolutions of the Deformed Woods-Saxon Potential via AIM. *Chin. Phys. Lett.* **30**, 020305.

[51] Kobos A M, Mackintosh R S 1982 Evaluation of model-independent optical potentials for the O^{16}+Ca^{40} system. *Phys. Rev.* **C26**, 1766-1769.

[52] Boztosun I 2002 New results in the analysis of O^{16}+Si^{28} elastic scattering by modifying the optical potential. *Phys. Rev.* **C66**, 024610.

[53] Boztosun I, Bayrak O, Dagdemir Y 2005 A Comparative study of the C^{12}+Mg^{24} system with deep and shallow potentials. *Int. J. Mod. Phys.* **E14**, 663-673.

[54] Kocak G, Karakoc M, Boztosun I, Balantekin A B 2010 Effects of α-cluster potentials for the O^{16}+O^{16} fusion reaction and S factor. *Phys. Rev.* **C81**, 024615.

[55] Dapo H, Boztosun I, Kocak G, Balantekin A B 2012 Influence of long-range effects on low-energy cross sections of He and HeX: The lithium problem. *Phys. Rev.* **C85**, 044602.

[56] Gamow G 1928 Zur Quantenheorie des Atomkernes *Z. Phys.* **51**, 204.

[57] Siegert A F J 1939 On the Derivation of the Dispersion Formula for Nuclear Reactions *Phys. Rev.* **56**, 750.

n	$E_n(MeV)$	n	$E_n(MeV)$	n	$E_n(MeV)$	n	$E_n(MeV)$
0	-75.283	6	-63.011	12	-39.441	18	-10.838
1	-74.336	7	-59.712	13	-34.806	19	-6.452
2	-72.873	8	-56.130	14	-30.050	20	-2.654
3	-70.967	9	-52.289	15	-25.213	21	-0.171
4	-68.665	10	-48.210	16	-20.347		
5	-66.004	11	-43.919	17	-15.522		

TABLE I. The energy spectrum of the α particle within Bohrium 270 nucleus under WS potential well assumption.

n	$E_n(MeV)$	n	$E_n(MeV)$	n	$E_n(MeV)$	n	$E_n(MeV)$
0	-75.166	6	-59.531	12	-29.605	17	$2.263 - 0.537 \times 10^{-3}i$
1	-73.915	7	-55.373	13	-23.607	18	$8.929 - 0.146 \times 10^{-1}i$
2	-72.022	8	-50.855	14	-17.386	19	$15.439 - 0.133i$
3	-69.585	9	-45.998	15	-10.971	20	$21.688 - 0.650i$
4	-66.666	10	-40.823	16	-4.402		
5	-63.304	11	-35.351				

TABLE II. The energy spectrum of the α particle within Bohrium 270 nucleus under GSWS potential well assumption. The rightmost column tabulates the quasi-bound energy levels.

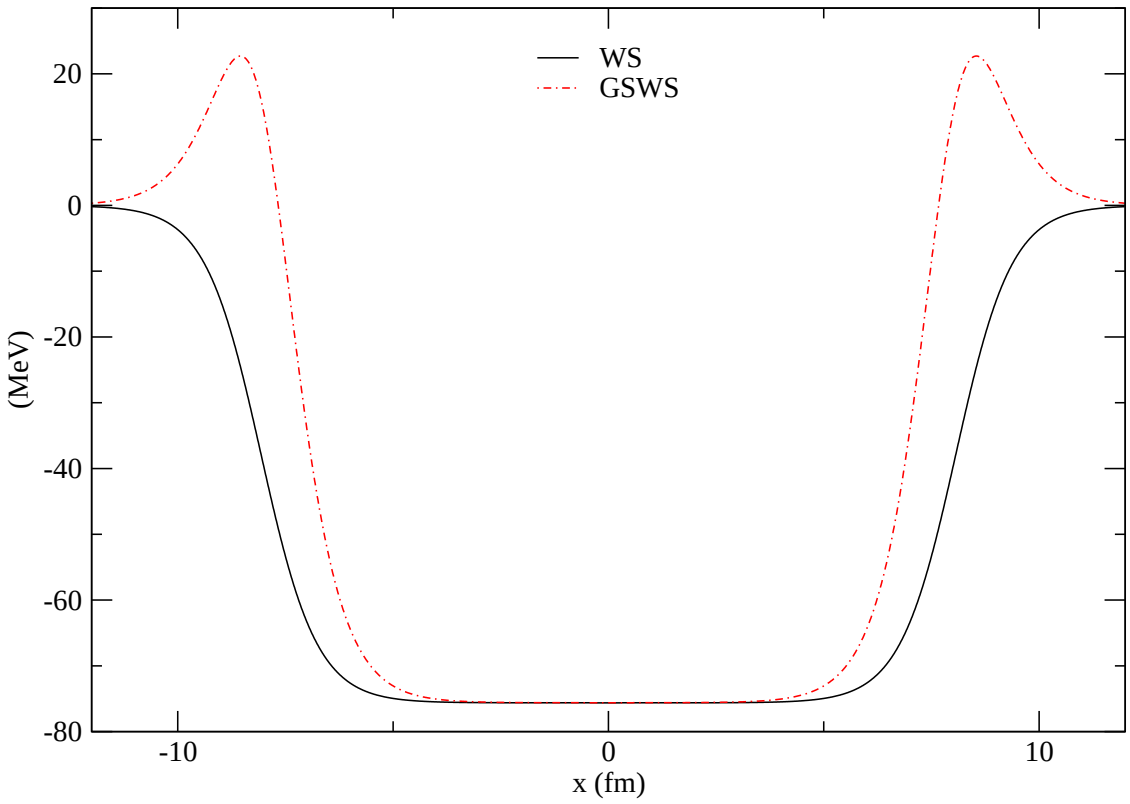

FIG. 1. The WS and GSWS potential well for an α-particle in a Bohrium 270 nucleus.

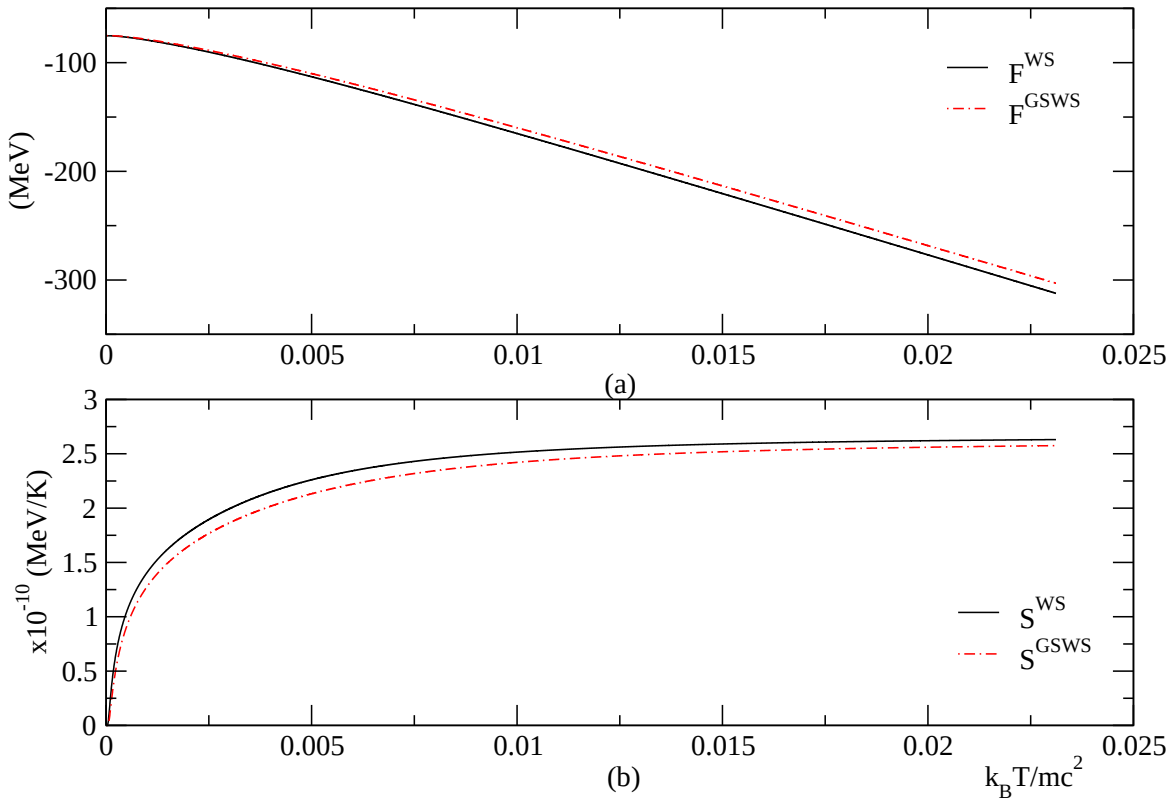

FIG. 2. Helmholtz energy $F(T)$ (a), entropy $S(T)$ (b), as functions of reduced temperature.

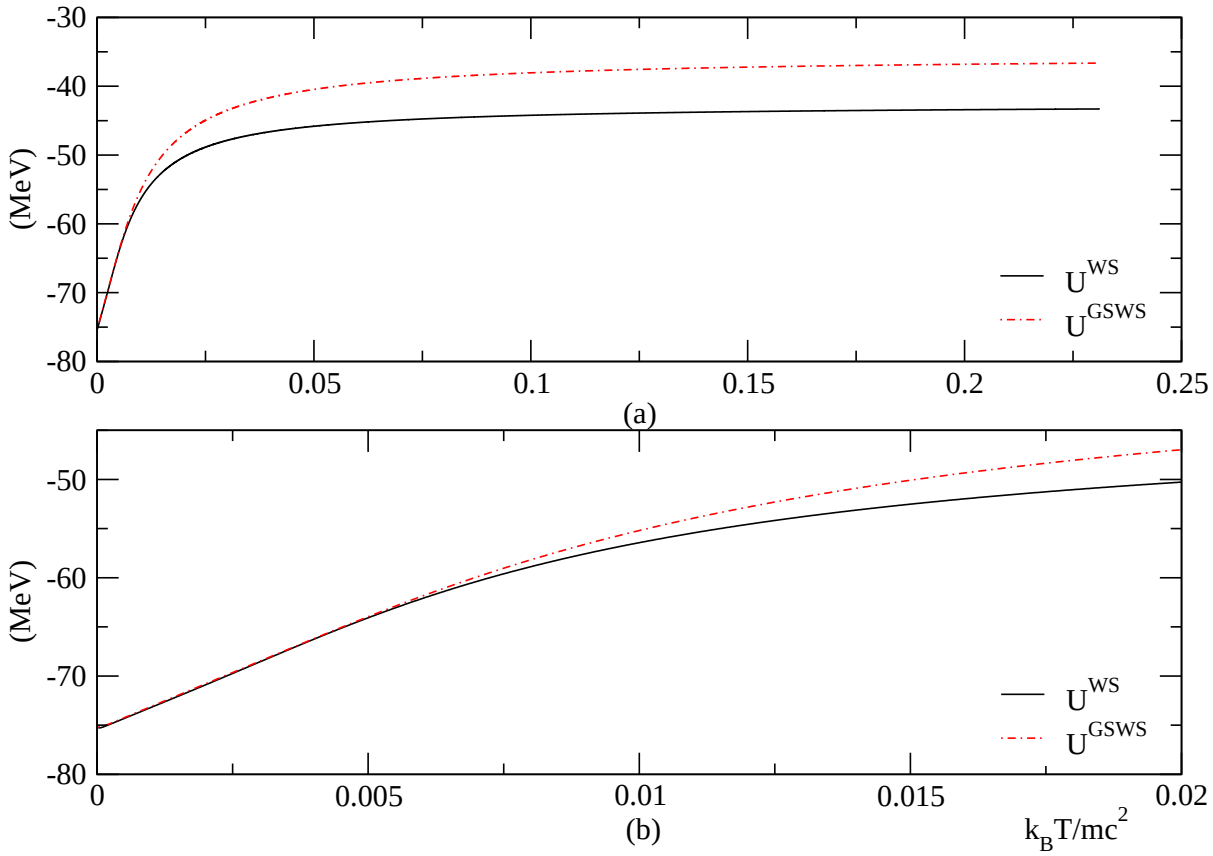

FIG. 3. Internal energy $U(T)$ as functions of reduced temperature (a), the initial behavior (b).

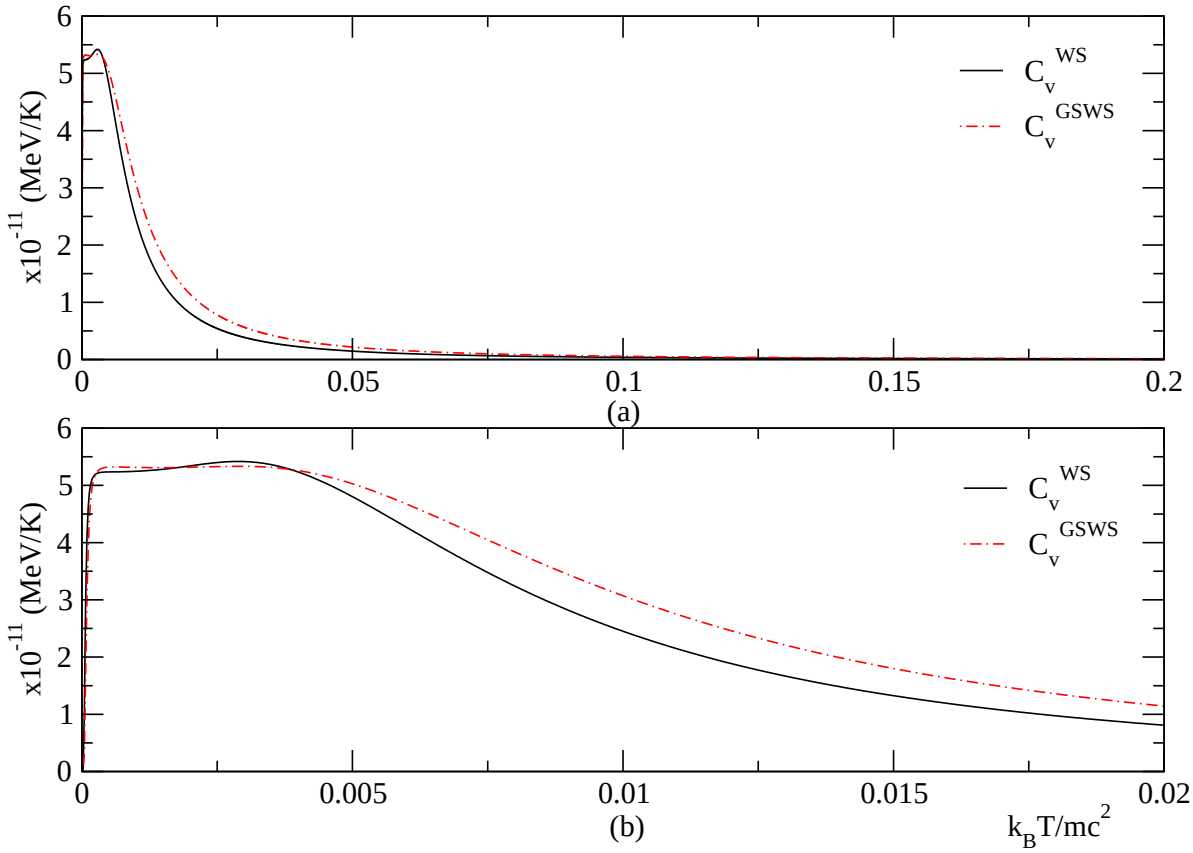

FIG. 4. Specific heat $C_v(T)$ as functions of reduced temperature (a), the initial behavior (b).